https://ntrs.nasa.gov/search.jsp?R=19700016402 2020-03-12T03:03:00+00:00Z

N70-25712
NASA CR-109619

MAGNETOHYDRODYNAMIC ROTATION IN AN ANNULUS

by

John P. Hanson and Ira M. Cohen

CASE FILE COPY

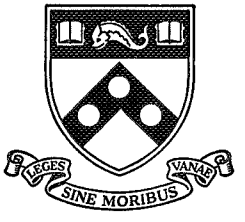

UNIVERSITY of PENNSYLVANIA

The Towne School
of
Civil and Mechanical Engineering

PHILADELPHIA, PENNSYLVANIA 19104

MAGNETOHYDRODYNAMIC ROTATION IN AN ANNULUS

by

John P. Hanson and Ira M. Cohen

INDEC - 80 January, 1970

This work has been supported by the Institute for Direct Energy Conversion under NASA Grant NsG-316 and NSF Grant GK-1847, and by The Towne School of Civil and Mechanical Engineering.
Reproduction in whole or in part is permitted for any purpose of the United States Government. Distribution of this document is limited.

Abstract

The problem of a liquid conductor confined between two concentric, perfectly conducting, cylindrical electrodes is considered. The liquid metal is electromagnetically accelerated by the Lorentz force in the circumferential direction created when a current I is passed between two electrodes and an axial magnetic induction field B_o is maintained. Asymptotic expansions are made in the smallness of the ratio of the magnetic Prandtl number ($\mathcal{P}_m$) and the smallness of the ratio of the magnetic induction created by the current I to that imposed by the magnet (B_o). Both parameters are small in a typical laboratory situation. In this limiting situation, nine asymptotically distinct regions are found: an inviscid main region in which the body force is balanced by convective acceleration, and viscous boundary layers on the inner and outer electrode surfaces, the top and bottom insulator surfaces, and four corner regions. It is shown that for the principal balance of effects over most of the domain, viscosity is unimportant but secondary flows are crucial. Although no solutions have been obtained, similarity laws are easily deduced and correlations are suggested. Preliminary experimental evidence tends to support these correlations.

In Appendix A we show that a contradiction is obtained if secondary flows are neglected. The conditions for which the secondary flow

decouples from the primary (circumferential) flow are derived in Appendix B and are those of creeping flow because of infinitesmal current flow.

Notation

(Rationalized MKS units are used throughout)

$\underset{\sim}{B}$ magnetic induction field (scalar components are denoted by subscripts appropriate for cylindrical coordinates)

$\underset{\sim}{E}$ electric field intensity

$\mathcal{E}$ $[2\pi r_1^3 \sigma^2 B_o^3/(\rho I)]^{1/2}$

$\underset{\sim}{g}$ acceleration due to gravity

$\mathcal{H}$ $B_o r_1 (\sigma/\eta)^{1/2}$ Hartmann number

I electric current

$\underset{\sim}{j}$ electric current density

$\mathcal{J}$ $\frac{\mu I}{2\pi}(\sigma/\eta)^{1/2}$

L axial length of device. $\hat{L} = L/r_1$

$\mathcal{M}$ $\mu I/(2\pi r_1 B_o)$

P gage pressure

$\mathcal{P}_m$ $\sigma\mu\eta/\rho$ magnetic Prandtl number

r radial coordinate. $r_{1,2}$ = radius of inner (outer) electrode

$\hat{r}_2 = r_2/r_1$

u,v,w stretched, dimensionless components of velocity in boundary regions

$\underset{\sim}{v}$ velocity of fluid (scalar components are denoted by subscripts appropriate for cylindrical coordinates)

z axial coordinate

ϵ electrical permittivity of fluid

ζ stretched dimensionless axial boundary layer coordinate

η dynamic viscosity of fluid

θ circumferential coordinate

μ magnetic permeability of fluid

ξ stretched dimensionless radial boundary layer coordinate

ρ mass density of fluid

ρ_e electric charge density of fluid measured in the laboratory frame

σ electrical conductivity of fluid

I. Introduction

An electrically conducting viscous liquid is confined in the annular volume bounded by two perfectly conducting coaxial cylindrical electrodes of radii r_1 and r_2 respectively, and length L as shown in Figure 1. The end closures are insulators, so an electric current passing between the electrodes must pass through the fluid. If an axial magnetic field is applied while a current is being passed between the electrodes, a circumferentially directed body force will result, causing the fluid to rotate. In general, the motion of the fluid is retarded by viscous effects, and steady state conditions are achieved when the momentum increase due to the body force is balanced by the frictional forces at the walls.

Two distinct mechanisms for achieving this balance of forces are possible, and one or the other may predominate depending upon the magnitude of the fluid velocity. One is that the velocity gradient at any given point is such that the local viscous forces just equal the body force at that point. This mode corresponds to "creeping flow" in ordinary fluid mechanics and occurs when the velocity is small. In the second mode, the electromagnetic force is balanced locally by the convective acceleration, which is, in turn, balanced by viscous forces in boundary layers near the walls. This mode, with the increase in fluid momentum being transported to viscous layers near the boundaries, predominates for large velocities.

In both cases, the motion of the fluid will distort the applied

magnetic field and the current distribution within the fluid. In general, the velocity, the current distribution, and the magnetic field cannot be decoupled and must be computed simultaneously. In order to reduce the equations describing these quantities to a more tractable form, a number of simplifying assumptions must be made. In addition to the assumptions that the electrodes are perfect conductors, that the end closures are perfect insulators, and that steady state has been achieved, all variables are assumed to be axially symmetric, and the fluid properties are assumed to be constants. The electric charge density is assumed to be negligible in Ohm's Law, and the electrical conductivity is assumed to be a scalar. Finally, the external magnetic field is assumed to be oriented in the axial direction and constant except for the distortions induced by the presence of currents in the device.

A number of investigators have attempted to calculate the flow using one or more assumptions in addition to those just listed. All of the works reviewed here have assumed the radial and axial components of velocity to be small in comparison with the tangential component, and many have assumed the radial current density at each electrode surface to be constant. The assumption of constant radial current density at the electrodes does not appear to lead to any difficulties in formulating the problem, although it imposes an additional constraint on any solution obtained. The assumption concerning the relative sizes of the tangential and secondary velocity

components must be treated with great care if a self-consistent formulation of the problem is to be obtained and, as it precludes the convection of momentum to the walls, it can only be applied for small velocities.

Gordeev and Gubanov[1] studied the flow near the center of a device whose length is much greater than any other dimension. As a consequence of geometry, they assumed that the radial component of the current and the velocity are functions of the radius only and are not influenced by the presence of the ends. Chang and Lundgren[2] investigated the one-dimensional flow of a liquid in a "short cylinder," a device whose radial dimensions are much greater than its length. They assumed the influence of the no-slip requirements at the electrodes to be negligible in the region away from the walls and assumed the velocity, the magnetic induction field, and the electric field could be written in the form $f(z)/r$. They also set the radial and axial components of velocity to zero, and proposed using the radial and axial components of the (conservation of) momentum equation to compute the pressure distribution in the fluid.

Lewellen[3], commenting on Chang and Lundgren's paper, pointed out that setting the secondary velocities identically equal to zero leads to a mathematical inconsistency for a viscous fluid. He indicated that perhaps the secondary flow could be treated as a small perturbation on an essentially one-dimensional flow field, but did not present the conditions for which this might be done. Gordeev[4], treated the one-dimensional case for a

general geometry with the implied assumption that the radial current density at each electrode is constant. Other researchers (cited in 5, 6 and 7) have presented various methods of solving the problem as formulated in References 1, 2, and 4, arriving at essentially similar results. In all of these papers, the flow is assumed to be one-dimensional, and in no case are the limitations of this assumption defined.

Although no conclusions can be drawn from the incomplete analysis presented by Erma and Podolsky[8], they do present experimental observations of the velocity and pressure distributions for a device which can be considered a "short cylinder." The velocity observed at a given point as a function of the current through the device and external magnetic induction field was compared with the analytical results obtained by previous investigators, and no correlation was found possible. A similar comparison was made with observations made at the University of Pennsylvania using a device with quite different proportions. For both sets of experimental data the velocity at a point was found to be proportional to the square root of the product of the external magnetic induction field and the current passing through the device. For large Hartmann numbers the velocity predicted in References 1, 4, and 5 for long cylinders is directly proportional to the product $B_0 I$. For long cylinders (References 2, 4, and 5) the predicted velocity is independent of the external field and directly proportional to the current for large Hartmann numbers. As the experimental Hartmann numbers were of the order of 100, these limiting behaviors would correlate with the observed behavior if the assumption of one-dimensional flow was valid.

This lack of correlation suggests that a more careful study is required of the flow configuration set up by the electromagnetic body force.

In the following the complete equations describing the three-dimensional flow field and the accompanying magnetic induction field will be derived under the assumptions previously mentioned. An approximation which is valid for velocities of the order of magnitude observed experimentally will be derived. In this approximation, the electromagnetic body force is not balanced locally by frictional forces, but the increase in momentum due to this force is convected to boundary layers near the walls where it is dissipated by friction. In addition to the inviscid main region where the convective acceleration balances the body force, eight viscous boundary regions on the four walls and in the four corners will be described.

The inconsistency pointed out by Lewellen[3] will be examined in Appendix A. A self-consistent formulation will be derived in Appendix B in which the equations and boundary conditions for v_θ and B_θ, used in references 1 through 7, for an assumed one-dimensional flow field, form an autonomous subsystem. In the derivation of this formulation, criteria limiting the size of the current and external field for which the one-dimensional approximation is valid will be found. Using these parameters, it will be shown that the one-dimensional approximation is valid only for extremely small fluid velocities.

II. Formulation of the Problem

The problem is completely described by Maxwell's equations, Ohm's law, the fluid mechanical conservation equations with a Lorentz body force and the appropriate boundary conditions. Under the assumptions made previously these can be written in the rationalized MKS system as:

$$\nabla \cdot \underset{\sim}{B} = 0 \tag{1}$$

$$\nabla \times \underset{\sim}{B} = \mu \underset{\sim}{j} \tag{2}$$

$$\nabla \times \underset{\sim}{E} = 0 \tag{3}$$

$$\nabla \cdot \underset{\sim}{E} = \rho_e / \epsilon \tag{4}$$

$$\underset{\sim}{j} = \sigma (\underset{\sim}{E} + \underset{\sim}{v} \times \underset{\sim}{B}) \tag{5}$$

$$\nabla \cdot \underset{\sim}{v} = 0 \tag{6}$$

$$\nabla (v^2/2) - \underset{\sim}{v} \times (\nabla \times \underset{\sim}{v}) = \nabla P/\rho + \underset{\sim}{j} \times \underset{\sim}{B}/\rho - (\nabla \times \nabla \times \underset{\sim}{v})\eta/\rho + \underset{\sim}{g} \tag{7}$$

Gauss' law (Equation (4)) is not necessary for the complete formulation of the problem, and can be used to find the charge density measured in the stationary reference frame. Although the fluid is assumed electrically neutral when observed from a reference frame moving with the fluid, ρ_e is not generally negligible, and setting it equal to zero would amount to making the unwarranted assumption that $\nabla \cdot (\underset{\sim}{v} \times \underset{\sim}{B}) = 0$. Although the charge density cannot be ignored in Gauss' law, order of magnitude arguments (as given by Shercliff[9] for example) show that it can be ignored in Ohm's law (Equation (5)).

The current density and the electric field intensity can be eliminated from these equations by direct substitution of Equation (2) and by taking the curl of Equation (5).

The resulting set is Eqs. (1) and (6) for conservation of magnetic flux and mass respectively, and

$$\nabla \times (\underset{\sim}{v} \times \underset{\sim}{B}) = \nabla \times (\nabla \times \underset{\sim}{B}) / \sigma\mu \quad , \qquad \text{magnetic equation} \tag{8}$$

$$\nabla (v^2/2) - \underset{\sim}{v} \times (\nabla \times \underset{\sim}{v}) = -\nabla P/\rho - \underset{\sim}{B} \times (\nabla \times \underset{\sim}{B})/\rho\mu - \nabla \times (\nabla \times \underset{\sim}{v})\eta/\rho + \underset{\sim}{g} \quad ,$$

$$\text{momentum equation} \tag{9}$$

The boundary conditions on these equations

$$v = 0 \quad \text{on all boundaries.} \tag{10}$$

$$\left.\begin{aligned} B_\theta &= 0 \quad \text{at} \quad z = L. \\ B_\theta &= \mu I/(2\pi r) \quad \text{at} \quad z = 0 \end{aligned}\right\} \tag{11}$$

$$\frac{\partial (rB_\theta)}{\partial r} = 0 \text{ at} \quad r = r_1 \text{ and } r = r_2. \tag{12}$$

$$\frac{\partial B_r}{\partial z} - \frac{\partial B_z}{\partial r} = 0 \quad \text{at } r = r_1 \text{ and } r = r_2 . \tag{13}$$

$$P = P_0 \quad \text{at } z = L \text{ and } r = r_1 . \tag{14}$$

B_r and B_z are continuous across all boundaries and B_z is specified on two z = constant surfaces (including the pole faces) and B_r is specified on a (distant) r = constant surface. (15)

Equation (10) is the usual no-slip condition for viscous fluid mechanics. Equation (11) represents the connections to the external current as

shown in Figure 1. These have been derived by the use of the integral form of Ampere's law $\oint \underset{\sim}{B} \cdot d\underset{\sim}{l} = \mu \int \underset{\sim}{j} \cdot d\underset{\sim}{s}$ and the condition of axial symmetry. Equation (12) states that $j_z = 0$ at the electrodes, and Equation (13) states that $j_\theta = 0$ on the electrodes. These are derived from Ohm's law, the no-slip condition on velocity, and the condition that the electric field intensity must be normal to the surface of a perfect conductor. Equation (14) allows the pressure to be defined in terms of the arbitrary reference pressure P_0. Equation (15) is a consequence of the lack of current sheets at the boundaries. In general the currents in the device will induce a B_r and B_z in addition to that present in the external field. In order to satisfy Equation (15), a transition solution to Ampere's law, Equation (2) with zero current, and the conservation of magnetic flux eqation, Equation (1), must be found in the region outside the device to match the external field with that induced in the de vice.

The radial and axial components of Equation (8) can be expanded as:

$$\frac{\partial}{\partial z}(v_z B_r - v_r B_z) = \frac{1}{\sigma\mu}\frac{\partial}{\partial z}\left(\frac{\partial B_r}{\partial z} - \frac{\partial B_z}{\partial r}\right) \tag{8a}$$

$$\frac{1}{r}\frac{\partial}{\partial r}\left[r(v_z B_r - v_r B_z)\right] = \frac{1}{\sigma\mu}\frac{1}{r}\frac{\partial}{\partial r}\left[r\left(\frac{\partial B_r}{\partial z} - \frac{\partial B_z}{\partial r}\right)\right] \tag{8b}$$

After integrating each of these once and applying Equations (10) and (13), the combined radial and axial components of the magnetic equation can be written as:

$$v_z B_r - v_r B_z = \frac{1}{\sigma\mu}\left(\frac{\partial B_r}{\partial z} - \frac{\partial B_z}{\partial r}\right) \tag{8c}$$

Equation (13) is no longer needed as a separate condition since it is satisfied identically by Equations (10) and (8c).

Equations (1), (6), (8), and (9) can be expanded in component form, and coupled with Equations (10), (11), (12), (14) and (15), provide the complete formulation of the problem.

$$\frac{1}{r}\frac{\partial}{\partial r}(rB_r) + \frac{\partial B}{\partial z}z = 0 \text{ , conservation of magnetix flux} \tag{1a}$$

$$\frac{1}{r}\frac{\partial}{\partial r}(rv_r) + \frac{\partial v}{\partial z}z = 0 \text{ , conservation of mass} \tag{6a}$$

$$v_z B_r - v_r B_z = \frac{1}{\sigma\mu}\left(\frac{\partial B_r}{\partial z} - \frac{\partial B}{\partial r}z\right) \text{ , radial-axial magnetic} \tag{8c}$$

$$\frac{\partial}{\partial z}(v_\theta B_z - B_\theta v_z) - \frac{\partial}{\partial r}(v_r B_\theta - v_\theta B_r) = -\frac{1}{\sigma\mu}\left[\frac{\partial}{\partial r}\frac{1}{r}\frac{\partial}{\partial r}(rB_\theta) + \frac{\partial^2 B}{\partial z^2}\theta\right], \tag{8d}$$

tangential magnetic

$$v_r\frac{\partial v}{\partial r}r + v_z\frac{\partial v}{\partial z}r - \frac{v^2}{r}\theta = -\frac{1}{\rho}\frac{\partial P}{\partial r} - \frac{1}{\rho\mu}\left[\frac{B_\theta}{r}\frac{\partial}{\partial r}(rB_\theta) - B_z\left(\frac{\partial B}{\partial z}r - \frac{\partial B}{\partial r}z\right)\right]$$

$$+ \frac{\eta}{\rho}\left[\frac{\partial}{\partial r}\frac{1}{r}\frac{\partial}{\partial r}(rv_r) + \frac{\partial^2 v}{\partial z^2}r\right] \text{ , radial momentum} \tag{9a}$$

$$\frac{v}{r}r\frac{\partial}{\partial r}(rv_\theta) + v_z\frac{\partial v}{\partial z}\theta = \frac{1}{\rho\mu}\left[\frac{B}{r}r\frac{\partial}{\partial r}(rB_\theta) + B_z\frac{\partial B}{\partial z}\theta\right]$$

$$+ \frac{\eta}{\rho}\left[\frac{\partial}{\partial r}\frac{1}{r}\frac{\partial}{\partial r}(rv_\theta) + \frac{\partial^2 v}{\partial z^2}\theta\right] \text{ , tangential momentum} \tag{9b}$$

$$v_r\frac{\partial v}{\partial r}z + v_z\frac{\partial v}{\partial z}z = -\frac{1}{\rho}\frac{\partial P}{\partial z} - \frac{1}{\rho\mu}\left[B_\theta\frac{\partial B}{\partial z}\theta + B_r\left(\frac{\partial B}{\partial z}r - \frac{\partial B}{\partial r}z\right)\right]$$

$$+ \frac{\eta}{\rho}\left[\frac{1}{r}\frac{\partial}{\partial r}\left(r\frac{\partial v}{\partial r}z\right) + \frac{\partial^2 v}{\partial z^2}z\right] - g \text{ , axial momentum} \tag{9c}$$

At this point it can be demonstrated that the additional assumption $v_r = v_z = 0$ leads to a contradiction. See Appendix A.

III. Asymptotic Analysis

A. Main Region

In order to simplify the governing equations, it is best to render them dimensionless so that relative sizes of terms can be compared. An appropriate normalization for the coordinate system can be obtained from the dimensions of the device. Equation (11) provides the normalization for B_θ. The scale factors for the remaining variables are not known a priori, and must be selected to retain the maximum number of terms in the equations under the expected operating conditions.[10] In comparing relative sizes of terms, the normalized parameters are assumed to be of order one. For this to be true in a region of finite extent, the normalized spatial derivatives of these quantities must also be of order one. Therefore, the relative sizes of the dimensionless parameters multiplying groups of terms serves as a measure of size. In obtaining the final balance, the properties of mercury were used, as well as 100 amperes as a typical current, 0.5 web./m^2 for the external magnetic induction field and 10^{-2} m. as a typical length.

The resulting dimensionless forms for the variables are as follows, as indicated by the caret notation.

$$\hat{\underset{\sim}{v}} = \left[\frac{2\pi r_1 \rho}{B_0 I}\right]^{1/2} \underset{\sim}{v}$$

$$\hat{B}_\theta = \frac{2\pi r_1}{\mu I} B_\theta$$

$$\hat{B}_r = \left[\frac{2\pi\rho}{\sigma^2 \mu^2 r_1 B_0^3 I}\right]^{1/2} B_r = \frac{B_r}{m B_0 \varepsilon}$$

$$\hat{B}_z = \left[\frac{2\pi\rho}{\sigma^2 \mu^2 r_1 B_0^3 I}\right]^{1/2} (B_z - B_0) = \frac{B_z - B_0}{m \varepsilon B_0}$$

$$\hat{P} = \frac{2\pi r_1}{B_0 I} (P + \rho g(z - L))$$

$$\hat{r} = r/r_1 \qquad 1 \leq \hat{r} \leq \hat{r}_2$$

$$\hat{z} = z/r_1 \qquad 0 \leq \hat{z} \leq \hat{L}$$

Five independent dimensionless parameters will appear in the equations, two describing the proportions of the device, and three more involving the properties of the fluid and the sizes of the current and the external magnetic induction field. Other dimensionless parameters are found from combinations of these five. The parameters follow, with typical sizes indicated:*

$$\hat{r}_2 = r_2/r_1 \qquad \hat{r}_2 = 6.52$$

$$\hat{L} = L/r_1 \qquad \hat{L} = 14.82$$

---

* The numerical values for these parameters are obtained from the dimensions of the particular device we have used and the range of current (10 - 100 amps.) and magnetic induction field (0.25 - 0.5 web/m^2) available to us.

$$\mathcal{E} = \left[\frac{2\pi r_1^3 \sigma^2 B_0^3}{\rho I}\right]^{1/2} \qquad .25 \leq \mathcal{E} \leq 2.5$$

$$\mathcal{M} = \frac{\mu I}{2\pi r_1 B_0} \qquad 4.38\times10^{-4} \leq \mathcal{M} \leq 8.76\times10^{-3}$$

$$P_m = \frac{\sigma \mu \eta}{\rho} \qquad P_m = 1.53\times10^{-7}$$

$$\mathcal{M}\mathcal{E} = \left(\frac{B_0 I}{2\pi r_1 \rho}\right)^{1/2} \sigma\mu r_1 \qquad 6.96\times10^{-4} \leq \mathcal{M}\mathcal{E} \leq 3.12\times10^{-3}$$

$$\frac{P_m}{\mathcal{M}\mathcal{E}} = \left(\frac{2\pi r_1 \rho}{B_0 I}\right)^{1/2} \frac{\eta}{r_1 \rho} \qquad 4.88\times10^{-5} \leq \frac{P_m}{\mathcal{M}\mathcal{E}} \leq 2.20\times10^{-4}$$

$$\mathcal{M}\mathcal{E}^2 = \frac{B_0^2 r_1^2 \sigma^2 \mu}{\rho} \qquad 5.54\times10^{-4} \leq \mathcal{M}\mathcal{E}^2 \leq 2.21\times10^{-3}$$

The parameter $\mathcal{E}$ is the ratio of the "back emf" induced by the fluid moving across the externally applied magnetic induction field to the voltage due to the electrical resistance of the fluid. For large values of $\mathcal{E}$, there will be large current sheets at the ends, while for decreasing values of $\mathcal{E}$, the radial component of current will vary more uniformly along the length of the device. $\mathcal{M}$ is the ratio of the magnetic induction field due to the current entering the device to the external field. For small values of $\mathcal{M}$ the Lorentz forces involving B_θ can be ignored. P_m is the magnetic Prandtl number, an index of relative thickness of viscous boundary layers compared with magnetic boundary layers. $\mathcal{M}\mathcal{E}$ can be seen to be the magnetic Reynolds number, the ratio of induced magnetic fields to applied fields. $P_m/\mathcal{M}\mathcal{E}$ is the inverse of the viscous Reynolds number, the ratio of viscous forces to inertial forces. $\mathcal{M}\mathcal{E}^2$ is the square of the Lundquist number. In

this problem it can be thought of as the product of $\mathcal{M}\mathcal{E}$ times $\mathcal{E}$, the ratio of the "back emf" generated by the motion of the fluid across the induced fields to the resistive voltage drop.

Figure 2 shows constant values of these parameters on a total current-magnetic induction field map. For the region of experimental interest $\mathcal{E}$ is of order one, and appropriate limits on the other parameters are $R_m \to 0$ and $\mathcal{M} \to 0$ so that $R_m/\mathcal{M}\mathcal{E} \to 0$. Figure 3 shows the limits on $\mathcal{M}$ and $\mathcal{E}$ for which these limits can be taken simultaneously. The viscous terms grow large in comparison with the convective acceleration, as the lower left corner is approached. Moving toward the right of this map, B_θ approaches B_0 in size. The top portion of this map represents the region where the voltage due to the resistivity of the fluid can be neglected in comparison with the "back emf." Suppressing the carets, the main region equations in these limits become:

$$\frac{1}{r}\frac{\partial}{\partial r}(rB_r) + \frac{\partial B_z}{\partial z} = 0 \qquad \text{conservation of magnetic flux} \qquad (16)$$

$$\frac{1}{r}\frac{\partial}{\partial r}(rv_r) + \frac{\partial v_z}{\partial z} = 0 \qquad \text{conservation of mass} \qquad (17)$$

$$v_r = \frac{\partial B_z}{\partial r} - \frac{\partial B_r}{\partial z} + O(\mathcal{M}\mathcal{E}) \qquad \text{radial-axial magnetic} \qquad (18)$$

$$\frac{\partial}{\partial r}\frac{1}{r}\frac{\partial}{\partial r}(rB_\theta) + \frac{\partial^2 B_\theta}{\partial z^2} = -\mathcal{E}\frac{\partial v_\theta}{\partial z} + O(\mathcal{M}\mathcal{E}) + O(\mathcal{M}\mathcal{E}^2)$$

$$\text{tangential magnetic} \qquad (19)$$

$$\frac{v_r}{r}\frac{\partial}{\partial r}(rv_\theta) + v_z\frac{\partial v_\theta}{\partial z} = \frac{\partial B_\theta}{\partial z} + O(R_m/\mathcal{M}\mathcal{E}) + O(\mathcal{M}\mathcal{E})$$

$$\text{tangential momentum} \qquad (20)$$

$$\frac{\partial P}{\partial r} = \frac{v_\theta^2}{r} - v_r \frac{\partial v_r}{\partial r} - v_z \frac{\partial v_r}{\partial z} + \mathcal{E} v_r + O(\mathcal{R}_m/\mathcal{M}\mathcal{E}) + O(\mathcal{M}) + O(\mathcal{M}\mathcal{E}^2)$$

radial momentum (21)

$$\frac{\partial P}{\partial z} = -v_r \frac{\partial v_z}{\partial r} - v_z \frac{\partial v_z}{\partial z} + O(\mathcal{R}_m/\mathcal{M}\mathcal{E}) + O(\mathcal{M}) + O(\mathcal{M}\mathcal{E}^2)$$

axial momentum (22)

Boundary conditions on these equations will be discussed after formulating the boundary region equations. Note that the problem for B_r and B_z has decoupled and may be solved from Equations (16) and (18) once the other variables are known.

B. Boundary Regions

As Equations (20), (21) and (22) do not include any frictional terms, there is no mechanism available for dissipating the increase in momentum due to the body forces. The convective acceleration terms provide a local balance, but in a closed system of finite dimensions they in turn must be balanced by frictional forces at the walls. There must, therefore, be thin regions near the walls where the derivatives of velocity are large so that the viscous terms become the same size as the convective acceleration. Eight of these boundary regions were found, two layers at the inner and outer electrodes, two layers at the top and bottom insulators, and four corner regions providing the transition between adjacent boundary layers. In addition, there are twelve overlap zones on the surfaces between adjacent regions where limiting solutions in both adjacent regions must have the same behavior if the dependent variables are to be continuous. These

zones are discussed in Reference 11. The locations of these regions are shown schematically in Figure 4.

In order to study the boundary regions the variables can be expanded in powers of the small parameter $R_m/m\mathcal{E}$. $R_m/m\mathcal{E}$ was selected for these expansions because the viscous terms must be recovered in the boundary regions to satisfy the boundary conditions for the complete problem. After expanding all the variables in arbitrary powers of $\frac{R_m}{m\mathcal{E}}$ the exponents were evaluated to retain the maximum number of terms in the boundary region equations and to satisfy the boundary conditions at the walls. In this process, the only requirements used were that the viscous terms be retained and that the maximum number of the remaining terms should be retained. The fact that the convective acceleration terms are retained indicates that the formulation is complete, and no new regions need to be found for $\mathcal{E}$ of order one.

The resulting expansions and equations for the top and bottom boundary layers are:

$$z = \left(R_m/m\mathcal{E}\right)^{1/2} \zeta_1$$

$$B_\theta = \frac{1}{r} + \left(\frac{R_m}{m\mathcal{E}}\right)^{\frac{1}{2}} B_\theta^{(1)}\,(r, \zeta_1)$$

in the bottom boundary layer.

$$z = L - \left(\frac{R_m}{m\mathcal{E}}\right)^{1/2} \zeta_2$$

$$B_\theta = \left(R_m/m\mathcal{E}\right)^{\frac{1}{2}} B_\theta^{(1)}\,(r, \zeta_2)$$

in the top boundary layer.

$$v_z = (R_m/m\varepsilon)^{1/2} w(r, \zeta_i), \qquad i = 1, 2$$

$$B_r = B_r^{(0)}(r) + (R_m/m\varepsilon)^{1/2} B_r^{(1)}(r, \zeta_i)$$

$$B_z = B_z^{(0)}(r) + (R_m/m\varepsilon)^{1/2} B_z^{(1)}(r, \zeta_i)$$

$$P = P^{(0)}(r) + \frac{R_m}{m\varepsilon} P^{(1)}(r, \zeta_i)$$

in both end boundary layers. In these regions v_r and v_θ do not change their scale.

To the order indicated, the resulting equations are as follows. Where the symbol $\pm$ or $\mp$ appears, the top symbol is to be used in the bottom boundary layer (ζ_1) and the bottom symbol for the top boundary layer (ζ_2).

$$\frac{1}{r}\frac{\partial}{\partial r}(r v_r) \pm \frac{\partial w}{\partial \zeta_i} = 0 \qquad \text{mass conservation} \qquad (23)$$

$$\frac{1}{r}\frac{\partial}{\partial r}(r B_r^{(0)}) \pm \frac{\partial B_z^{(1)}}{\partial \zeta_i} = 0 \qquad \text{conservation of magnetic flux} \qquad (24)$$

$$v_r = \frac{\partial B_z^{(0)}}{\partial r} \mp \frac{\partial B_r^{(1)}}{\partial \zeta_i} + O[(R_m/m\varepsilon)^{1/2}] + O(m\varepsilon) + O[m\varepsilon(R_m/m\varepsilon)^{1/2}]$$

radial-axial magnetic (25)

$$\frac{\partial^2 B_\theta^{(1)}}{\partial \zeta_i^2} = \mp \varepsilon \frac{\partial v_\theta}{\partial \zeta_i} + O(R_m/m\varepsilon) + O(m\varepsilon^2) + O[m\varepsilon^2(R_m/m\varepsilon)^{1/2}]$$

tangential magnetic (26)

$$v_r \frac{\partial v_\theta}{\partial r} \pm w \frac{\partial v_\theta}{\partial \zeta_i} = \frac{\partial B_\theta^{(1)}}{\partial \zeta_i} \frac{\partial^2 v_\theta}{\partial \zeta_i^2} + O(R_m/m\varepsilon) + O[m\varepsilon(R_m/m\varepsilon)^{1/2}]$$

tangential momentum (27)

$$\frac{\partial P^{(0)}}{\partial r} = \frac{v_\theta^2}{r} - v_r \frac{\partial v_r}{\partial r} \mp w \frac{\partial v_r}{\partial \zeta_i} = \mathcal{E} v_r + \frac{\partial^2 v_r}{\partial \zeta^2} + O(\rho_m/m\mathcal{E}) + O[m(\rho_m/m\mathcal{E})] + O(m\mathcal{E}^2)$$

radial momentum (28)

$$\frac{\partial P^{(1)}}{\partial \zeta_i} = \mp v_r \frac{\partial w}{\partial r} - w \frac{\partial w}{\partial \zeta_i} \pm \frac{\partial^2 w}{\partial \zeta_i^2} + O[(\rho_m/m\mathcal{E})^2] + O[m(\rho_m/m\mathcal{E})^{1/2}] + O[m\mathcal{E}^2(\rho_m/m\mathcal{E})^{1/2}]$$

axial momentum (29)

The boundary conditions on these equations are that all velocities as well as the higher order terms $B_\theta^{(1)}$, $B_r^{(1)}$, $B_z^{(1)}$ and $P^{(1)}$ must be zero at $\zeta_i = 0$. As v_θ and v_r do not change scaling through the boundary layers they must remain finite as $\zeta_i \to \infty$. As $\zeta_i \to \infty$, all variables must match the solutions obtained in the main region as well as match the corner region solutions as $r \to 1$ and $r \to r_2$.

A similar procedure can be used to obtain the boundary layer equations for the inner and outer boundary layers. The resulting expansions and equations are:

$r = 1 + \xi_1 (\rho_m/m\mathcal{E})^{1/2}$ in the inner boundary layer

$r = r_2 - \xi_2 (\rho_m/m\mathcal{E})^{1/2}$ in the outer boundary layer

$$v_r = \left(\frac{\rho_m}{m\mathcal{E}}\right)^{1/2} u$$

$$B_r = B_r^{(0)}(z) + (\rho_m/m\mathcal{E})^{1/2} B_r^{(1)}(\xi_i, z), \qquad i = 1, 2$$

$$B_\theta = B_\theta^{(0)}(z)\left[1 \mp \left(\frac{\rho_m}{m\mathcal{E}}\right)^{\frac{1}{2}} \xi_i + \frac{\rho_m}{m\mathcal{E}} \xi_i^2\right] + \frac{\rho_m}{m\mathcal{E}} B_\theta^{(1)}(\xi_i, z)$$

$$B_z = B_z^{(0)}(z) + \left(\frac{\rho_m}{m\mathcal{E}}\right)^{\frac{1}{2}} B_z^{(1)}(\xi_i, z)$$

$$P = P^{(0)}(z) + \left(\frac{\rho_m}{m\mathcal{E}}\right)^{\frac{1}{2}} P^{(1)}(\xi_i, z)$$

$$\pm \frac{\partial B_r^{(1)}}{\partial \xi_i} + B_r^{(0)} + \frac{\partial B^{(0)}}{\partial z} z = O\left((R_m/m\varepsilon)^{1/2}\right)$$

conservation of magnetic flux (30)

$$\frac{\partial u}{\partial \xi_i} + \frac{\partial v}{\partial z} z = O\left((R_m/m\varepsilon)^{1/2}\right)$$

conservation of mass (31)

$$\frac{\partial B_r^{(o)}}{\partial z} \mp \frac{\partial B_z^{(1)}}{\partial \xi_i} = O\left((R_m/m\varepsilon)^{1/2}\right)$$

radial-axial magnetic (32)

$$\frac{\partial^2 B_\theta^{(1)}}{\partial \xi_i^2} + \frac{\partial^2 B_\theta^{(0)}}{\partial z^2} = -\varepsilon \frac{\partial v}{\partial z}\theta \mp \left(m^2\varepsilon^5/R_m\right)^{\frac{1}{2}} B_r^{(o)} \frac{\partial v}{\partial \xi_i}\theta + O\left[(R_m/m\varepsilon)^{1/2}\right] + O(m\varepsilon)$$

tangential magnetic (33)

$$\mp u \frac{\partial v}{\partial \xi_i}\theta + v_z \frac{\partial v}{\partial z}\theta = \frac{\partial B}{\partial z}\theta^{(0)} + \frac{\partial^2 v}{\partial \xi_i^2}\theta + O\left((R_m/m\varepsilon)^{1/2}\right) + O(m\varepsilon)$$

tangential momentum (34)

$$\pm \frac{\partial P^{(1)}}{\partial \xi_i} = v_\theta^2 + O\left((R_m/m\varepsilon)^{1/2}\right) + O(m)$$

radial momentum (35)

$$\frac{\partial P^{(o)}}{\partial z} = \mp u \frac{\partial v}{\partial \xi_i} z - v_z \frac{\partial v}{\partial z} z + \frac{\partial^2 v}{\partial \xi_i^2} z + O\left((R_m/m\varepsilon)^{1/2}\right) + O(m)$$

axial momentum (36)

The boundary conditions on these equations are similar to those for the end boundary layers. The velocities and higher order terms in the expansions must go to zero on the walls, and all variables must match with the adjacent regions in the overlap zones.

The corner regions which provide the transition between the side and end boundary layers must be small in r and in z. A similar procedure

of scaling in terms of powers of $(R_m/m\mathcal{E})$ and attempting to select the powers to retain the greatest number of terms can be used.

In these regions the following scalings and equations are obtained. The indices i and j each take on the value of 1 or 2 depending on which corner is under consideration. For the bottom two corners j = 1, while i = 1 denotes the inside and i = 2 the outside. The relations for the top two corners are obtained with j = 2 , and the values of i indicating inner and outer regions as before.

$r = 1 + \xi_1 (R_m/m\mathcal{E})^{1/2}$ in the inner two corner regions

$r = r_2 - \xi_2 (R_m/m\mathcal{E})^{1/2}$ in the outer two corner regions

$z = \left(\frac{R_m}{m\mathcal{E}}\right)^{\frac{1}{2}} \zeta_1$ in the bottom two corner regions

$z = L - (R_m/m\mathcal{E})^{\frac{1}{2}} \zeta_2$ in the top two corner regions

$v_r = (R_m/m\mathcal{E})^{\frac{1}{2}} u \quad , \qquad v_\theta = (R_m/m\mathcal{E})^{\frac{1}{2}} v \qquad v_z = (R_m/m\mathcal{E})^{\frac{1}{2}} w$

$$B_r = B_r^{(0)} + (R_m/m\mathcal{E})^{\frac{1}{2}} B_r^{(1)} \quad (\xi_i, \zeta_j)$$

$$B_\theta = B_\theta^{(0)} \left[1 + (-1)^i \xi_i (R_m/m\mathcal{E})^{\frac{1}{2}} + \xi_i^2 (R_m/m\mathcal{E}) \right] + (R_m/m\mathcal{E})^{3/4} B_\theta^{(1)} (\xi_i, \zeta_i)$$

$$B_z = B_z^{(0)} + (R_m/m\mathcal{E})^{\frac{1}{2}} B_z^{(1)} (\xi_i, \zeta_i)$$

$$P = P^{(0)} + (R_m/m\mathcal{E}) P^{(1)} (\xi_i, \zeta_i)$$

$P^{(0)}$, $B_r^{(0)}$ and $B_z^{(0)}$ are constants which will have different values in each of the corner regions, to match the values at the appropriate corners of the main region. $B_\theta^{(0)} = 0$ in the top two corner regions from Equation (11). Similarly $B_\theta^{(0)} = 1$ in the inner bottom corner region and $B_\theta^{(0)} = 1/r_2$ in the outer bottom corner region from Equation (11). The equations are:

$$(-1)^i \frac{\partial B_r^{(1)}}{\partial \xi_i} - B_r^{(0)} + (-1)^j \frac{\partial B_z^{(1)}}{\partial \zeta_j} = O((\mathcal{R}_m/m\mathcal{E})^{1/2})$$

conservation of magnetic flux (37)

$$(-1)^i \frac{\partial u}{\partial \xi_i} + (-1)^j \frac{\partial w}{\partial \zeta_j} = O((\mathcal{R}_m/m\mathcal{E})^{1/2})$$

conservation of mass (38)

$$(-1)^i \frac{\partial B_z^{(1)}}{\partial \xi_i} - (-1)^j \frac{\partial B_r^{(1)}}{\partial \zeta_j} = O((\mathcal{R}_m/m\mathcal{E})^{1/2})$$

radial-axial magnetic (39)

$$\frac{\partial^2 B_\theta^{(1)}}{\partial \xi_i^2} + \frac{\partial^2 B_\theta^{(1)}}{\partial \zeta_j^2} = (-1)^j \mathcal{E} \frac{\partial v}{\partial \zeta_j} + O[(m\mathcal{E}^2)] + O[(\mathcal{R}_m/m\mathcal{E})^{1/4}]$$

tangential magnetic (40)

$$(-1)^i u \frac{\partial v}{\partial \xi_i} + (-1)^j w \frac{\partial v}{\partial \zeta_j} = (-1)^j \frac{\partial B_\theta^{(1)}}{\partial \zeta_j} - \frac{\partial^2 v}{\partial \xi_i} - \frac{\partial^2 v}{\partial \zeta_j} + (m\mathcal{E})^{3/4} \mathcal{R}_m^{-1/4} B_r^{(0)} B_\theta^{(0)} + O[(\mathcal{R}_m/m\mathcal{E})^{1/2}]$$

tangential momentum (41)

$$(-1)^i \frac{\partial P^{(1)}}{\partial \xi_i} = -v^2 - (-1)^i u \frac{\partial u}{\partial \xi_i} - (-1)^j w \frac{\partial u}{\partial \zeta_j} - \mathcal{E} u - \frac{\partial^2 u}{\partial \xi_i^2} - \frac{\partial^2 u}{\partial \zeta_j^2} + O(m\mathcal{E}^2) + O[m(\mathcal{R}_m/m\mathcal{E})^{1/4}]$$

radial momentum (42)

$$(-1)^j \frac{\partial P^{(1)}}{\partial \zeta_j} = - (-1)^i \; u \frac{\partial w}{\partial \xi_i} - (-1)^j \; w \frac{\partial w}{\partial \zeta_j} - \frac{\partial^2 w}{\partial \xi_i^2} - \frac{\partial^2 w}{\partial \zeta_j^2}$$

$$+ O(m\varepsilon^2) + O[m(\rho_m / m\varepsilon)^{1/4}]_{\text{axial momentum}} \qquad (43)$$

Again velocities and higher order terms in the expansions must be zero on the walls, and solutions must match those obtained in adjacent regions in the overlap zones.

C. Main Region Boundary Conditions

With the formulation of the boundary layer equations complete, the boundary conditions on the main region equations can be examined. As the variation in B_θ has been shown to be small in the boundary regions, the boundary conditions on B_θ that apply at the walls will carry over into the main region. The normal components of velocity are also small in the boundary regions. To within the order indicated by the scaling of the dependent variables in the boundary regions, the boundary conditions for the main region are Equation (15) for B_r and B_z, and

$$v_z(r,0) = v_z(r,L) = v_r(1,z) = v_r(r_2, z) = 0$$

$$B_\theta(r, 0) = 1/r$$

$$B_\theta(r, L) = 0$$

$$\frac{\partial}{\partial r}(rB_\theta) = 0 \text{ at } r = 1, r_2$$

Note that there are no boundary conditions on v_θ. However, we believe that the main region problem is well formulated. There is

a sufficient number of equations and boundary conditions for an adequate formulation of the complete problem, (as will be demonstrated in Appendix B for the slow flow (one-dimensional) case), and the boundary region equations appear to be properly formulated.

From the boundary condition on the secondary velocities in the main region, the conservation of mass equation, and the requirements that velocities be continuous, there must be at least one point in the main region where $v_r = v_z = 0$ simultaneously. At this point, the radial component of current $(-\partial B_\theta/\partial z)$ must also be zero from the tangential momentum equation. It is expected that the radial current will vary smoothly over the length of the device, and be of order one in most of the main region for moderate or small values of $\mathcal{E}$.

D. Subsidiary Limits

In the limit, as $\mathcal{E} \to 0$, Equation (19) reduces to the form it would have if the velocity was zero. The solution to this equation is $B_\theta = (L - z)/Lr$. As this solution cannot satisfy Equation (20) at the point where v_r and v_z are zero simultaneously, an additional asymptotic region must appear for the limiting case as $\mathcal{E} \to 0$. In this region, derivatives must be large enough to enable $\partial B_\theta/\partial z$ to go to zero at this point where v_r and v_z are zero.

In the other extreme, as $\mathcal{E} \to \infty$, $\partial v_\theta/\partial z$ and $\partial B_\theta/\partial z$ approach zero throughout the entire main region. These two quantities will both be large in the

the end boundary layers, resulting in the formation of Hartmann layers.

In this extreme Equations (16) through (22) must be rescaled to retain a maximum balance. The new scaled variables (indicated by the tilde notation) can be defined in terms of the old scaled variables (caret) used for moderate or small values of $\mathcal{E}$

$$\tilde{\underset{\sim}{v}} = \mathcal{E}\hat{\underset{\sim}{v}} = \frac{2\pi r_1 \sigma B_0}{I} \quad \underset{\sim}{v}$$

$$\tilde{B}_r = \mathcal{E}\hat{B}_r = \frac{2\pi r_1}{\mu I} \quad B_r$$

$$\tilde{B}_z = \mathcal{E}\hat{B}_z = \frac{2\pi r_1}{\mu I} \quad (B_0 - B_z)$$

$$\tilde{P} = \mathcal{E}^1\hat{P} = \frac{4\pi^2 r_1^4 \sigma^2 B_0^2}{\rho I^2} \left[p + \rho g(z-L)\right]$$

$$\tilde{B}_\theta = \hat{B}_\theta = \frac{2\pi r_1}{\mu I} \quad B_\theta$$

Equations (16) and (17) do not change in form. The remaining equations for the main region are:

$$\frac{\partial}{\partial r}\frac{1}{r}\frac{\partial}{\partial r}(r\tilde{B}_\theta) + \frac{\partial^2 \tilde{B}}{\partial z^2}\theta = -\frac{\partial \tilde{v}}{\partial z}\theta + O(\mathcal{M})$$
tangential magnetic (44)

$$\frac{\tilde{v}_r}{r}\frac{\partial}{\partial r}(r\tilde{v}_\theta) + \tilde{v}_z\frac{\partial \tilde{v}}{\partial z}\theta = \mathcal{E}^2\frac{\partial \tilde{B}}{\partial z}\theta + O(R_m/\mathcal{M}) + O(\mathcal{M}\mathcal{E})$$
tangential momentum (45)

$$\frac{\partial \tilde{P}}{\partial r} = \frac{\tilde{v}^2}{r}\theta - \tilde{v}_r\frac{\partial \tilde{v}_r}{\partial r} - \tilde{v}_z\frac{\partial \tilde{v}_r}{\partial z} + \tilde{v}_r + O(R_m/\mathcal{M}) + O(\mathcal{M}\mathcal{E})$$
radial momentum (46)

$$\frac{\partial \tilde{P}}{\partial z} = -\tilde{v}_r\frac{\partial \tilde{v}_z}{\partial r} - \tilde{v}_z\frac{\partial \tilde{v}_z}{\partial z} + O(R_m/\mathcal{M}) + O(\mathcal{M}\mathcal{E})$$
axial momentum (47)

IV. Comparison with Experiment

Although the system of equations describing the flow has not been solved, some conclusions can be drawn concerning the behavior of the flow by inspection of the equations. The only parameter appearing explicitly in the main region equations is $\mathcal{E}$.

At any given point, therefore, the normalized velocity and pressure is expected to be only a function of $\mathcal{E}$ and the geometric parameters $\hat{L}$ and $\hat{r}_2$, to the order of the terms neglected. Velocity measurements as shown in Figure 5 tend to support this conclusion. As the device used by Erma and Podolsky[8] is of quite different proportions ($\hat{r}_2 = 4$, $\hat{L} = 1$) than that used at the University of Pennsylvania ($\hat{r}_2 = 6.25$, $\hat{L} = 14.82$) the two sets of data are not expected to have the same numerical values. The trends of both sets of data indicates that not only is v_θ a function of $\mathcal{E}$ only, but that it is a weak function of $\mathcal{E}$ over the range $0.2 < \mathcal{E} < 2.0$.

Measurements of the pressure distribution in the top plane of the device at the University of Pennsylvania shown in Figure 6 indicate that the normalized radial pressure gradient varies only slightly with current and magnetic field over most of the gap width. Measurements of the pressure difference between two points in this region are shown on an expanded scale as a function of $\mathcal{E}$ in Figure 7. Again, the normalized pressure difference appears to be primarily a function of $\mathcal{E}$ only. All of these observations tend to confirm the ability of the analytic formulation to adequately represent the experiments.

Attempts to measure the direction of flow were not nearly as satisfactory. Measurements made of the ratio v_r/v_θ near the bottom of the device indicated that this ratio tends to increase with the magnetic field for a constant value of $\mathcal{E}$. Measurements of the ratio v_z/v_θ as a function of radius, current and magnetic field proved to be not reproducible. In general the size of this ratio was large near the electrodes, but the sign varied between successive experiments. Once a particular flow pattern was established, it persisted for as long as the device was kept in continuous operation. Stopping the device for a period of time and then restarting it generally led to the establishment of a new pattern, however.

As values for the ratios v_r/v_θ and v_z/v_θ as large as 0.2 were observed, the existence of a significant secondary flow field was confirmed. The measurements of v_z/v_θ seem to confirm the existence of secondary flow cells, but also indicate that a number of different cell arrangements may be stable once established. Apparently, the establishment of any given cell arrangement is quite dependent on comparatively small effects, and it seems unreasonable to suppose that the location of instrumentation probes would not influence the configuration established. Therefore obtaining comparable measurements of flow direction at different axial locations will be difficult unless a means of controlling the cell arrangements is established.

The device occupies a comparatively small portion of the volume between the pole faces, and the variation of the axial magnetic induction

field is less than 2% of the centerline average throughout the volume actually enclosed by the device. Small as this variation is, it still is much larger than that induced by the tangential currents in the device, and may have an appreciable influence on the character of the secondary flow. This inhomogeniety in the external field may explain the behavior observed in the ratio v_r/v_θ.

V. Conclusions

The problem of an electromagnetically accelerated liquid conductor confined between two concentric, perfectly conducting, cylindrical electrodes was considered. Asymptotic expansions were made in the smallness of the magnetic Prandtl number ($\mathcal{P}_m$) and the smallness of the ratio of the magnetic induction created by the current I to that imposed by the magnet (B_o). Both parameters were shown to be small in a typical laboratory situation. In this limiting situation, nine asymptotically distinct regions were found: an inviscid main region in which the body force was balanced by convective acceleration, and viscous boundary layers on the inner and outer electrode surfaces, the top and bottom insulator surfaces, and four corner regions. It was shown that for the principal balance of effects over most of the domain, viscosity is unimportant but secondary flows are crucial. Although no solutions were obtained, similarity laws were easily deduced and correlations were suggested. Preliminary experimental evidence tended to support these correlations.

In Appendix A we show that a contradiction is obtained if secondary flows are neglected. The conditions for which the secondary flow decouples from the primary (circumferential) flow are derived in Appendix B and are those of creeping flow because of infinitesmal current flow.

Appendix A: Contradiction Obtained by Neglecting Secondary Flow

If secondary flows are neglected, i.e., $v_r = v_z = 0$, then Equation (8c) becomes:

$$\frac{\partial B_r}{\partial z} - \frac{\partial B_z}{\partial r} = 0 \qquad (A-1)$$

Equations (9a) and (9c) then become:

$$\frac{\partial P}{\partial r} = \rho \frac{v_\theta^2}{r} - \frac{1}{\mu} \frac{B_\theta}{r} \frac{\partial (r B_\theta)}{\partial r} \qquad (A-2)$$

$$\frac{\partial P}{\partial z} = - \frac{B_\theta}{\mu} \frac{\partial B_\theta}{\partial z} - \rho g \qquad (A-3)$$

Solving (A-3) for P

$$P = - \frac{1}{2\mu} B_\theta^2 - \rho g z + f(r), \qquad (A-4)$$

where f (r) is an arbitrary function of the radius only. After substituting this into Equation (A - 2) we obtain:

$$r \frac{df(r)}{dr} = \rho v_\theta^2 - \frac{1}{\mu} B_\theta^2$$

The left hand side of this expression is a function of the radius only, and the relation must hold for any position within the device. Selecting the surface of the inner electrode ($r = r_1$) to evaluate the expression, $v_\theta = 0$ from Equation (10) and $r \frac{df(r)}{dr} = C$. The relationship can now be written as:

$$C = - \frac{1}{\mu} B_\theta^2 (r_1). \qquad (A-6)$$

From Equation (11), $B_\theta(r_1)$ is not a constant, and the secondary velocity cannot be ignored in the formulation of the problem. As $j_r = \frac{1}{\mu}\frac{\partial B_\theta}{\partial z}$ this demonstration is not restricted to problems of finite length, but can be applied to the "long cylinder" case as well. The assumption of perfect electrodes, constant fluid properties, axial symmetry, steady state conditions, and the presence of a radial component of current are sufficient to require the inclusion of the secondary components of velocity in the calculations.

Appendix B: One-Dimensional Flow Analysis

For low flow velocities, the electromagnetic body forces can be balanced locally by the viscous terms. By forcing this balance on Equations (1a), (6a), (8c), (8d), (9a), (9b), and (9c), a set of parameters can be derived which must be small if the body forces are to be balanced locally by the viscous terms. In deriving these parameters, the magnetic Prandtl number ($\mathcal{P}_m$) was assumed to be of order one or smaller. As the magnetic Prandtl number is large only for highly ionized plasmas, and the assumptions of constant properties and scalar conductivity would not be valid in this case, the restriction to moderate values of $\mathcal{P}_m$ does not affect the generality of the results. In developing this formulation, the Hartmann number based on the axial magnetic induction field was assumed to be of order one, and no boundary layers appear in the resulting approximate equations. These equations are shown to be valid for quite large axial Hartmann numbers, and Hartmann layers do appear for this condition. The dimensionless forms (indicated by the carets) are:

$$\hat{v}_\theta = \frac{2\pi r_1 \sqrt{\sigma\eta}}{I^1} v_\theta$$

$$\left.\begin{matrix}\hat{v}_r \\ \hat{v}_z\end{matrix}\right\} = \frac{4\pi^2 r_1 \sigma\eta^2}{\rho I^2} \left\{\begin{matrix}v_r \\ v_z\end{matrix}\right.$$

$$\left.\begin{matrix}\hat{B}_r \\ \hat{B}_z\end{matrix}\right\} = \frac{4\pi^2\eta^2}{\rho\mu I^2} \left\{\begin{matrix}B_r \\ B_z\end{matrix}\right. - B_0$$

$$\hat{P} = \frac{4\pi^2 r_1^2 \sigma\eta}{\rho I^2}\left[P + \rho g(z - L)\right]$$

The following dimensionless parameters can be defined in addition to $\hat{L}$ and $\hat{r}_2$:

$$\mathcal{H} = B_0 r_1 \sqrt{\sigma/\eta} = (m\mathcal{E}^2/\mathcal{P}_m)^{1/2}$$

$$\mathcal{J} = \frac{\mu I}{2\pi}\sqrt{\sigma/\eta} = (m^3\mathcal{E}^2/\mathcal{P}_m)^{1/2}$$

$$\mathcal{P}_m = \sigma\mu\eta/\rho$$

$\mathcal{H}$ is the Hartmann number based on the axial magnetic induction field, and $\mathcal{J}$ the Hartmann number based on the tangential field.

Dropping the caret notation, Equations (1a), (6a), (8c), (8d), (9a), (9b), and (9c) can be written as:

$$\frac{1}{r}\frac{\partial}{\partial r}(rv_r) + \frac{\partial v_z}{\partial z} = 0 \qquad \text{conservation of mass} \qquad \text{(B-1)}$$

$$\frac{1}{r}\frac{\partial}{\partial r}(rB_r) + \frac{\partial B_z}{\partial z} = 0 \qquad \text{conservation of magnetic flux} \qquad \text{(B-2)}$$

$$v_r = \left(\frac{\partial B_z}{\partial r} - \frac{\partial B_r}{\partial z}\right) - \frac{\mathcal{J}^2}{\mathcal{P}_m}(v_r B_z - v_z B_r)$$

axial-radial magnetic (B-3)

$$\frac{\partial}{\partial r}\frac{1}{r}\frac{\partial}{\partial r}(rB_\theta) + \frac{\partial^2 B_\theta}{\partial z^2} = -\mathcal{H}\frac{\partial v_\theta}{\partial z} - \frac{\mathcal{J}^2}{\mathcal{P}_m}\left[\frac{\partial}{\partial z}(B_\theta v_z) + \frac{\partial}{\partial r}(B_\theta v_r)\right]$$

$$+ \frac{\mathcal{J}^2\mathcal{H}}{\mathcal{P}_m}\left[\frac{\partial}{\partial z}(v_\theta B_z) + \frac{\partial}{\partial r}(v_\theta B_r)\right] \quad \text{tangential magnetic} \qquad \text{(B-4)}$$

$$\frac{\partial}{\partial r}\frac{1}{r}\frac{\partial}{\partial r}(rv_\theta) + \frac{\partial^2 v_\theta}{\partial z^2} = -\mathcal{H}\frac{\partial B_\theta}{\partial z} - \frac{\mathcal{J}^2\mathcal{H}}{\mathcal{P}_m}\left[\frac{B_r}{r}\frac{\partial}{\partial r}(rB_\theta) + B_z\frac{\partial B_\theta}{\partial z}\right]$$

$$- \frac{\mathcal{J}^2}{\mathcal{P}_m^2}\left[\frac{v_r}{r}\frac{\partial}{\partial r}(rv_\theta) + v_z\frac{\partial v_\theta}{\partial z}\right] \text{tangential momentum} \qquad \text{(B-5)}$$

$$\frac{\partial P}{\partial r} = \frac{v_\theta^2}{r} + \frac{\partial}{\partial r}\frac{1}{r}\frac{\partial (rv_r)}{\partial r} + \frac{\partial^2 v_r}{\partial z^2} - \mathcal{H}^2\left(\frac{\partial B_r}{\partial z} - \frac{\partial B_z}{\partial r}\right)$$

$$+ \mathcal{R}_m \frac{B_\theta}{r}\frac{\partial}{\partial r}(rB_\theta) - \frac{\mathcal{H}^2 J^2}{\mathcal{R}_m} B_z\left[\frac{\partial B_r}{\partial z} - \frac{\partial B_z}{\partial r}\right]$$

$$- \frac{J^2}{\mathcal{R}_m^2}\left[v_r \frac{\partial v_r}{\partial r} + v_z \frac{\partial v_r}{\partial z}\right] \quad \text{radial momentum} \qquad \text{(B-6)}$$

$$\frac{\partial P}{\partial z} = \frac{1}{r}\frac{\partial}{\partial r}\left(r \frac{\partial v_z}{\partial r}\right) + \frac{\partial^2 v_z}{\partial z^2} - \mathcal{R}_m B_\theta \frac{\partial B_\theta}{\partial z} - \frac{J^2 \mathcal{H}^2}{\mathcal{R}_m} B_r\left(\frac{\partial B_r}{\partial z} - \frac{\partial B_z}{\partial r}\right)$$

$$- \frac{J^2}{\mathcal{R}_m^2}\left[v_r \frac{\partial v_z}{\partial r} + v_z \frac{\partial v_z}{\partial z}\right] \quad \text{axial momentum} \qquad \text{(B-7)}$$

By inspection, the two sets of conditions can be determined for which the viscous terms dominate the convective acceleration terms:

For $\mathcal{H} > 1$,

$$J \ll \mathcal{R}_m$$

$$\mathcal{H} \ll \mathcal{R}_m / J^2$$

The first defines the maximum current for which the viscous terms predominate in the momentum equations while the second defines the maximum external field for which the induced fields can be neglected.

The maximum value of $\mathcal{E}$ and $\mathcal{M}$ for which these conditions can be met simultaneously for mercury are indicated in the lower left corner of Figure 3.

For $\mathcal{H} < 1$, the two independent conditions reduce to one:

$$J^2 \ll \mathcal{R}_m^2 \mathcal{H}.$$

These two conditions can be seen to be equivalent for $\mathcal{H} = 1$ and $\mathcal{R}_m$ of order one or smaller.

If these conditions are met, Equations (B-3) through (B-7) can be written to the order indicated as:

$$v_r = \frac{\partial B_z}{\partial r} - \frac{\partial B_r}{\partial z} + O(\mathcal{J}^2/\mathcal{R}_m)$$

axial-radial magnetic (B-3a)

$$\frac{\partial}{\partial r}\frac{1}{r}\frac{\partial}{\partial r}(rB_\theta) + \frac{\partial^2 B_\theta}{\partial z^2} = -\mathcal{H}\frac{\partial v_\theta}{\partial z} + O(\mathcal{J}^2/\mathcal{R}_m) + O(\mathcal{J}^2\mathcal{H}/\mathcal{R}_m)$$

tangential magnetic (B-4a)

$$\frac{\partial}{\partial r}\frac{1}{r}\frac{\partial}{\partial r}(rv_\theta) + \frac{\partial^2 v_\theta}{\partial z^2} = -\mathcal{H}\frac{\partial B_\theta}{\partial z} + O(\mathcal{J}^2\mathcal{H}/\mathcal{R}_m) + O(\mathcal{J}^2/\mathcal{R}_m^2)$$

tangential momentum (B-5a)

$$\frac{\partial P}{\partial r} = \frac{v_\theta^2}{r} + \frac{\partial}{\partial r}\frac{1}{r}\frac{\partial}{\partial r}(rv_r) + \frac{\partial^2 v_r}{\partial z^2} - \mathcal{H}^2 v_r + \mathcal{R}_m\frac{B_\theta}{r}\frac{\partial}{\partial r}(rB_\theta)$$

$$+ O(\mathcal{J}^2/\mathcal{R}_m^2) + O(\mathcal{R}_m\mathcal{H})$$ radial momentum (B-62)

$$\frac{\partial P}{\partial z} = \frac{1}{r}\frac{\partial}{\partial r}\left(r\frac{\partial v_z}{\partial r}\right) + \frac{\partial^2 v_z}{\partial z^2} - \mathcal{R}_m B_\theta\frac{\partial B_\theta}{\partial z} + O(\mathcal{R}_m\mathcal{H}) + O(\mathcal{J}^2/\mathcal{R}_m^2)$$

axial momentum (B-7a)

The boundary conditions on these equations are Equations (10), (11), (12), (14), and (15) for the complete problem with Equation (11) written as $B_\theta(r,0) = 1/r$ in scaled form.

Equations (B-4a) and (B-5a), and Equations (10), (11) and (12) are equivalent to the systems solved in References 1 through 7 for one-dimensional flow, and their computed values for v_θ and B_θ apply directly. The secondary velocities can be written in terms of partial derivatives of a stream function Ψ, and Equations (B-1), (B-6a) and (B-7a) reduce to a single linear inhomogenous fourth order partial differential equation

with a known forcing function. The boundary conditions on this equation are that Ψ and its normal derivatives be zero on the boundaries. Once the secondary velocity is known, Equations (B-2) and (B-3a) can be solved with Equation (15) for the induced fields. Equations (B-1), (B-2), and (B-3a) through (B-7a) with Equations (10), (11), (12), (14), and (15) have been shown to constitute a well formulated representation of the complete problem for low velocity flows. As the low velocity approximation is of the same derivative order as the complete problem, these boundary conditions must be sufficient for a well formulated system for the high velocity representation.

For most liquid metals R_m is much smaller than one, and the terms involving B_θ in Equations (B-6a) and (B-7a) can be neglected. Assuming that N is greater than one, the error in Equations (B-3a) through (B-7a) is less than 10% if $J < 4.7 \times 10^{-8}$ and $H < 6.5 \times 10^{6}$ for mercury ($R_m = 1.53 \times 10^{-7}$). This condition on J is shown in Figure 3 along with the conditions for which the three-dimensional equations are valid. These restrictions are equivalent to requiring that the current be less than 10^{-5} amperes, and the axial magnetic induction field be less than 2×10^{3} web/m^2, for $r_1 = 10^{-2}$ m. The tangential velocity corresponding to these conditions is of the order of 4×10^{-6} m/sec. As this current and corresponding velocity is much smaller than those of experimental interest, it is not surprising that the results obtained in References 1 through 7 have not been observed experimentally.

References:

1. Gordeev, G. V. and Gubanov, A. I., "Acceleration of a Plasma in a Magnetic Field," Sov. Phys. - Tech. Phys., 3, 1880 - 1887, (1958).

2. Chang, C. C. and Lundgren, T. S., "Flow of an Incompressible Fluid in a Hydromagnetic Capacitor," Phys. Fluids, 2, 627-632, (1959).

3. Lewellen, W. S., "Comment on The Flow of an Incompressible Fluid in a Hydromagnetic Capacitor," Phys. Fluids, 5, 1663-1664, (1962).

4. Gordeev, G. V., "The Nonstationary Rotation of a Plasma in a Magnetic Field," Sov. Phys.- Tech. Phys., 6, 195-202, (1961).

5. Kessey, K. O., "Rotating Electrically Conducting Fluids in a Long Cylinder," A. I. A.A.J., 2, 864-871, (1964).

6. Kessey, K. O., "Magnetohydrodynamic Rotation of Plasmas," Ph.D. Dissertation, Columbia University, 1963.

7. Schweitzer, S. and Soler, A. I., "One Dimensional Viscous Magnetohydrodynamic Flow in an Annulus," A.I.A.A. Paper 69-725, 1964.

8. Erma, V.A. and Podalsky, B., "A Fundamental Theoretical and Experimental Study of Rotary Magnetohydrodynamics," Plasmadyne Corp. Final Report, Contract A F 49(638) - 1149, Project-Task 9752-01 for Air Force Office of Scientific Research, 1964. (Defense Documentation Center AD 609812)

9. Shercliff, J. A. A Textbook of Magnetohydrodynamics (Pergamon Press, New York, 1965).

10. Kruskal, M.D., "Asymptotology," in Mathematical Models in Physical Sciences, S. Drobot, Ed. (Prentice-Hall, Inc., Englewood Cliffs, New Jersey, 1963).

11. Hanson, J.P., "Magnetohydrodynamic Rotation of a Conducting Liquid in an Annulus," Ph. D. Dissertation, University of Pennsylvania, 1970.

Figure Captions:

1. MHD Device and Coordinate System
2. Current-Magnetic Field Map for Mercury
3. Parameter Map for Mercury
4. Location of Asymptotic Regions
5. Normalized Velocity as a Function of $\mathcal{E}$
6. Typical Normalized Pressure Distribution
7. Normalized Pressure as a Function of $\mathcal{E}$

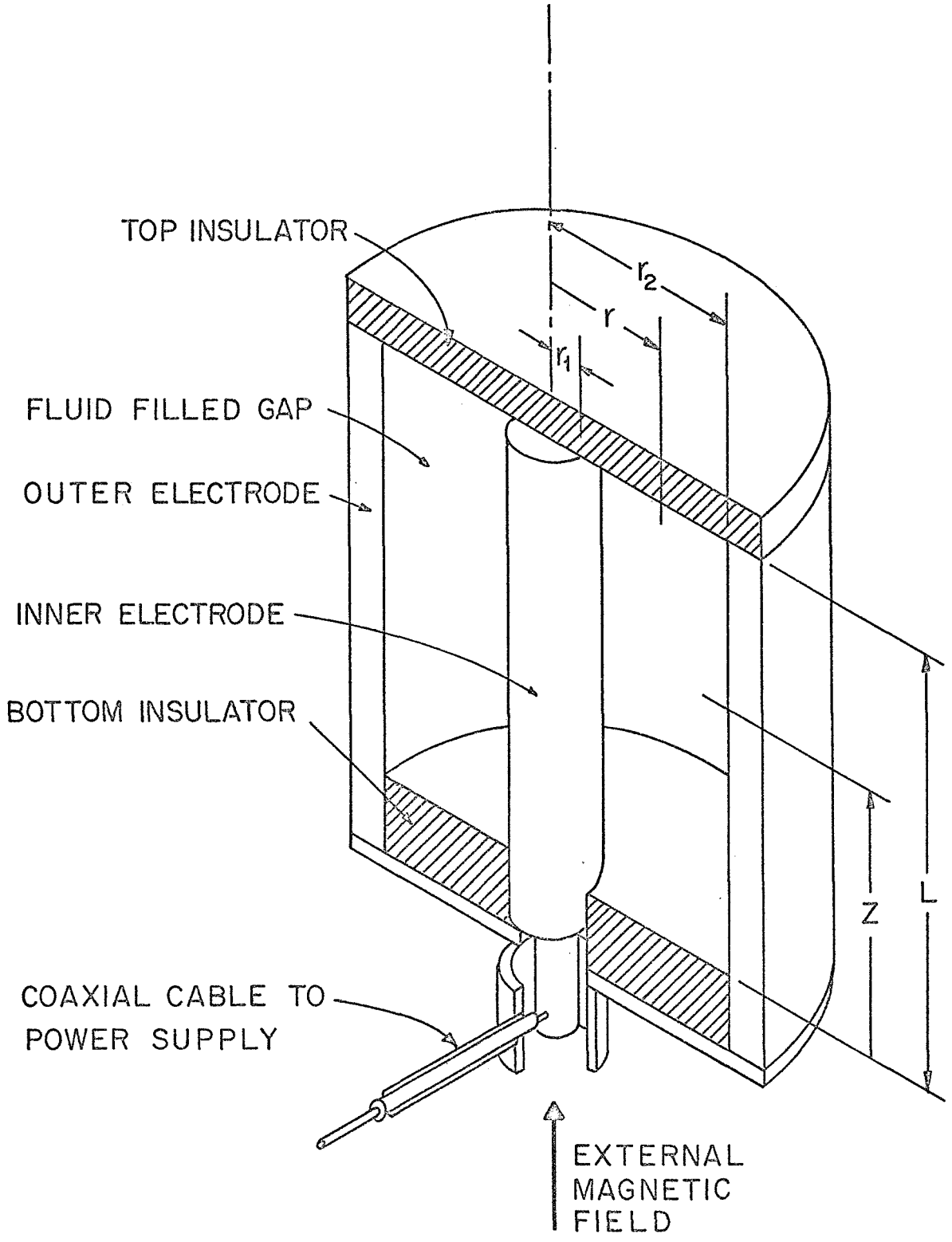

MHD DEVICE AND COORDINATE SYSTEM

FIG. 1

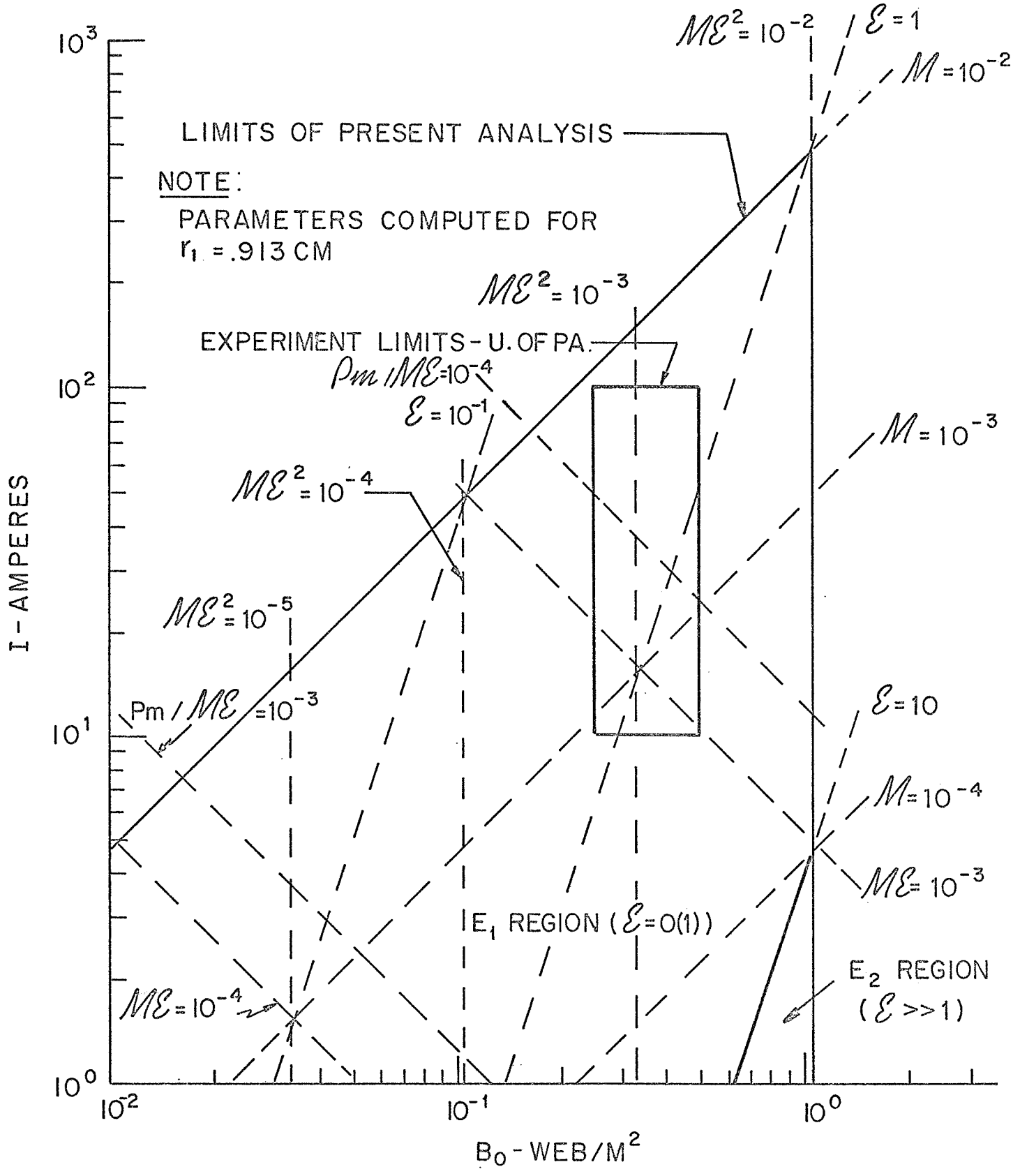
10^3
10^2
10^1
10^0
I - AMPERES
10^{-2}
10^{-1}
10^0
B_0 - WEB/M^2
$M\mathcal{E}^2 = 10^{-2}$
$\mathcal{E} = 1$
$M = 10^{-2}$
LIMITS OF PRESENT ANALYSIS
NOTE:
PARAMETERS COMPUTED FOR
r_1 = .913 CM
$M\mathcal{E}^2 = 10^{-3}$
EXPERIMENT LIMITS - U. OF PA.
$Pm/M\mathcal{E} = 10^{-4}$
$\mathcal{E} = 10^{-1}$
$M = 10^{-3}$
$M\mathcal{E}^2 = 10^{-4}$
$M\mathcal{E}^2 = 10^{-5}$
$Pm/M\mathcal{E} = 10^{-3}$
$\mathcal{E} = 10$
$M = 10^{-4}$
$M\mathcal{E} = 10^{-3}$
E_1 REGION ($\mathcal{E}$ = O(1))
$M\mathcal{E} = 10^{-4}$
E_2 REGION
($\mathcal{E} >> 1$)

FIG. 2

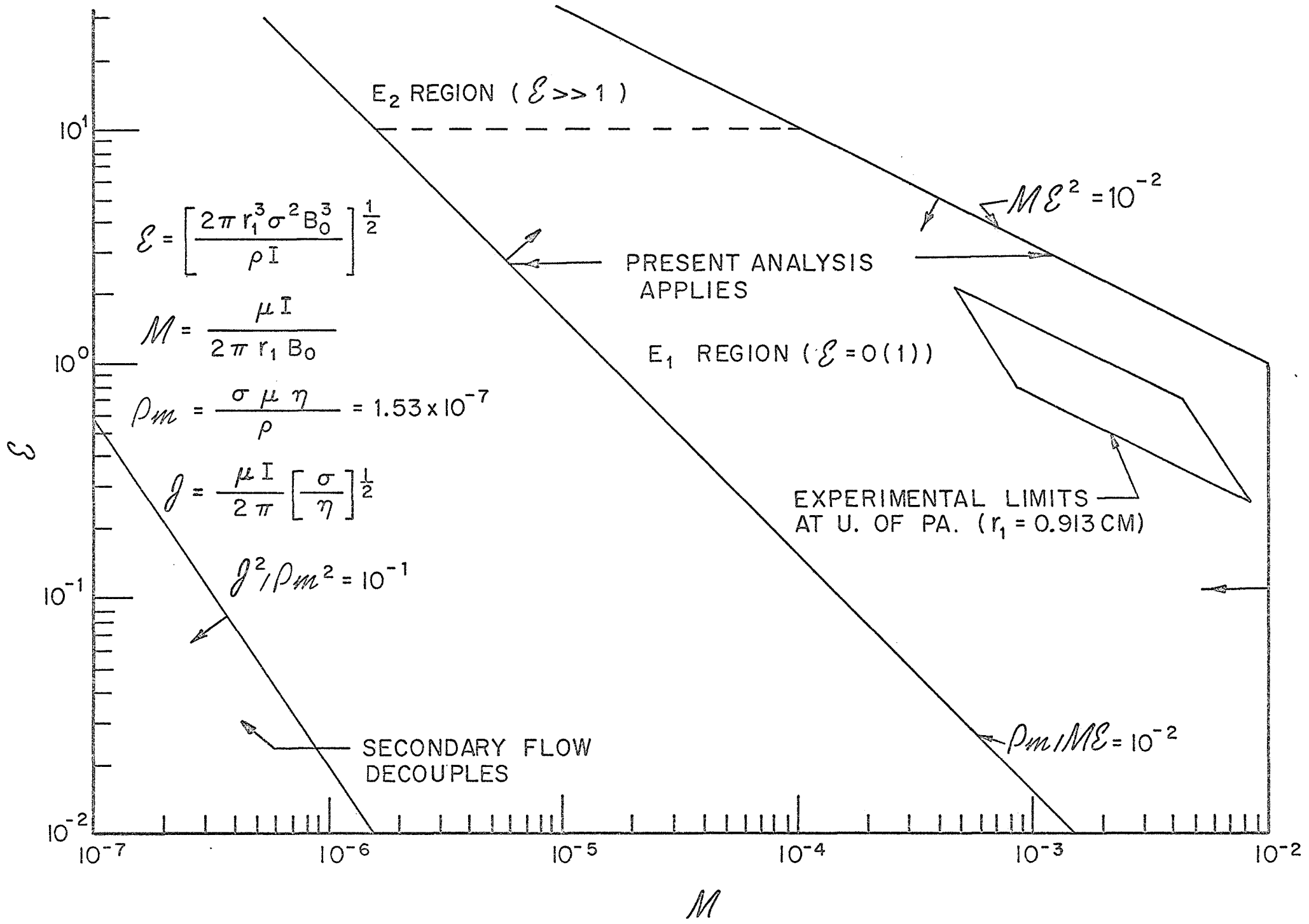
E2 REGION (ℰ >> 1)
$\mathcal{E} = \left[\frac{2\pi r_1^3 \sigma^2 B_0^3}{\rho I}\right]^{\frac{1}{2}}$
$M = \frac{\mu I}{2\pi r_1 B_0}$
$\rho_m = \frac{\sigma \mu \eta}{\rho} = 1.53 \times 10^{-7}$
$J = \frac{\mu I}{2\pi}\left[\frac{\sigma}{\eta}\right]^{\frac{1}{2}}$
$J^2/\rho_m^2 = 10^{-1}$
$M\mathcal{E}^2 = 10^{-2}$
PRESENT ANALYSIS APPLIES
E1 REGION (ℰ = O(1))
EXPERIMENTAL LIMITS AT U. OF PA. (r1 = 0.913 CM)
SECONDARY FLOW DECOUPLES
$\rho_m/M\mathcal{E} = 10^{-2}$
10^1
10^0
10^{-1}
10^{-2}
10^{-7}
10^{-6}
10^{-5}
10^{-4}
10^{-3}
10^{-2}
ℰ
M

FIG. 3

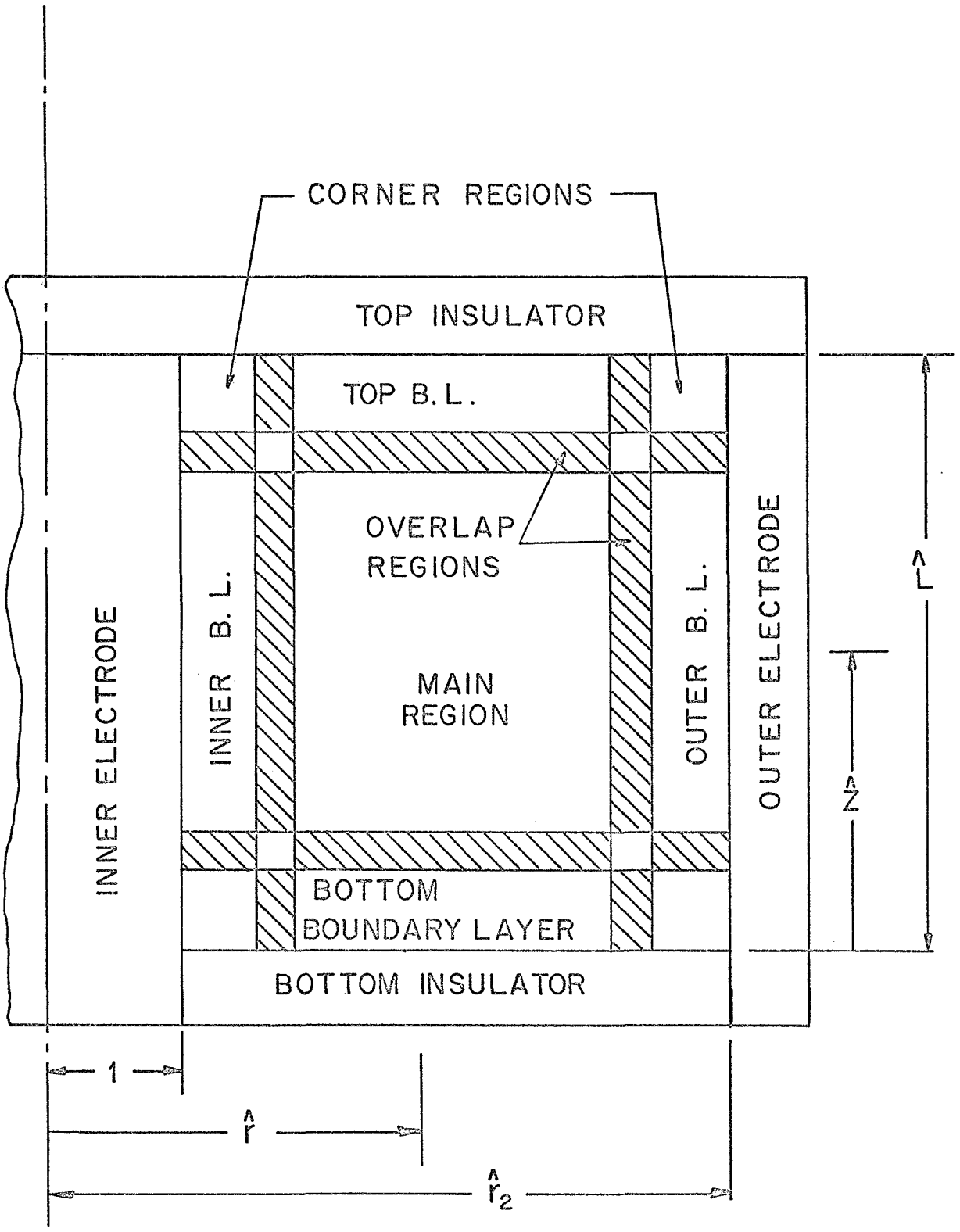

LOCATION OF ASYMPTOTIC REGIONS

FIG. 4

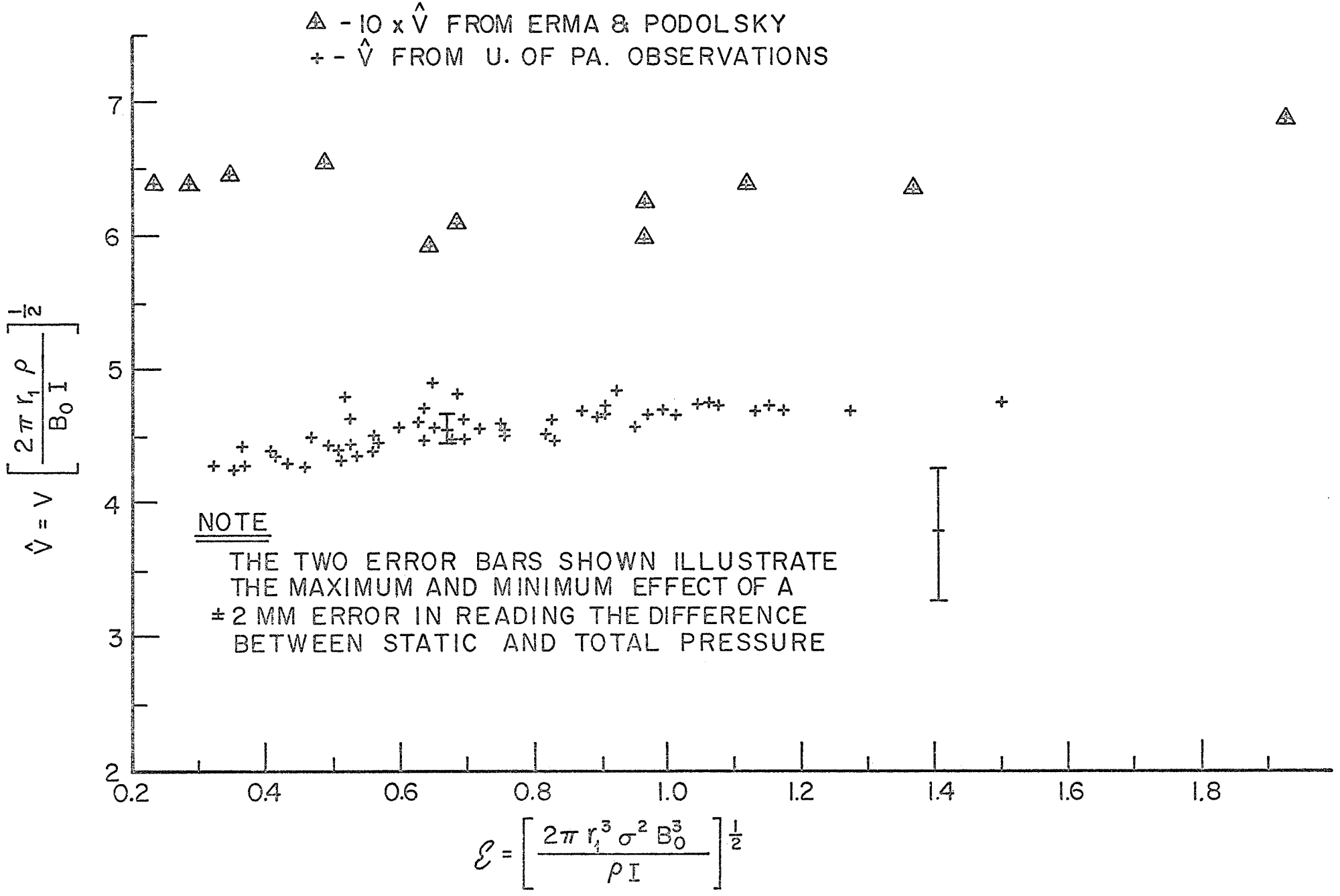
△ - 10 x V̂ FROM ERMA & PODOLSKY
+ - V̂ FROM U. OF PA. OBSERVATIONS
NOTE
THE TWO ERROR BARS SHOWN ILLUSTRATE THE MAXIMUM AND MINIMUM EFFECT OF A ±2 MM ERROR IN READING THE DIFFERENCE BETWEEN STATIC AND TOTAL PRESSURE
$\hat{V} = V \left[\frac{2\pi r_1 \rho}{B_0 I}\right]^{\frac{1}{2}}$
$\mathcal{E} = \left[\frac{2\pi r_1^3 \sigma^2 B_0^3}{\rho I}\right]^{\frac{1}{2}}$
2
3
4
5
6
7
0.2
0.4
0.6
0.8
1.0
1.2
1.4
1.6
1.8

FIG. 5

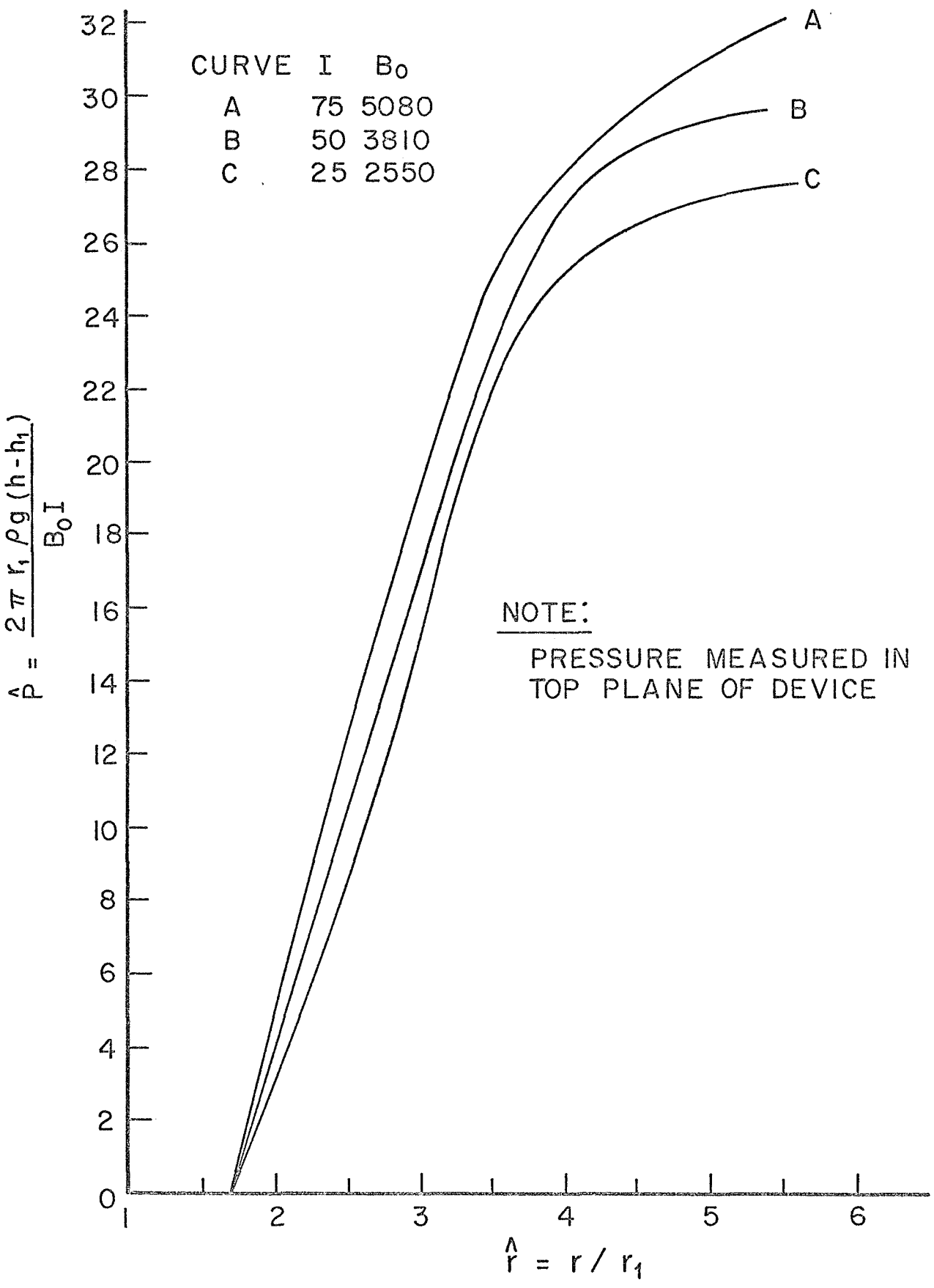
CURVE I Bo
A 75 5080
B 50 3810
C 25 2550
A
B
C
NOTE:
PRESSURE MEASURED IN TOP PLANE OF DEVICE
$\hat{P} = \frac{2\pi r_1 \rho g (h-h_1)}{B_0 I}$
$\hat{r} = r / r_1$
0
2
4
6
8
10
12
14
16
18
20
22
24
26
28
30
32
1
2
3
4
5
6

FIG. 6

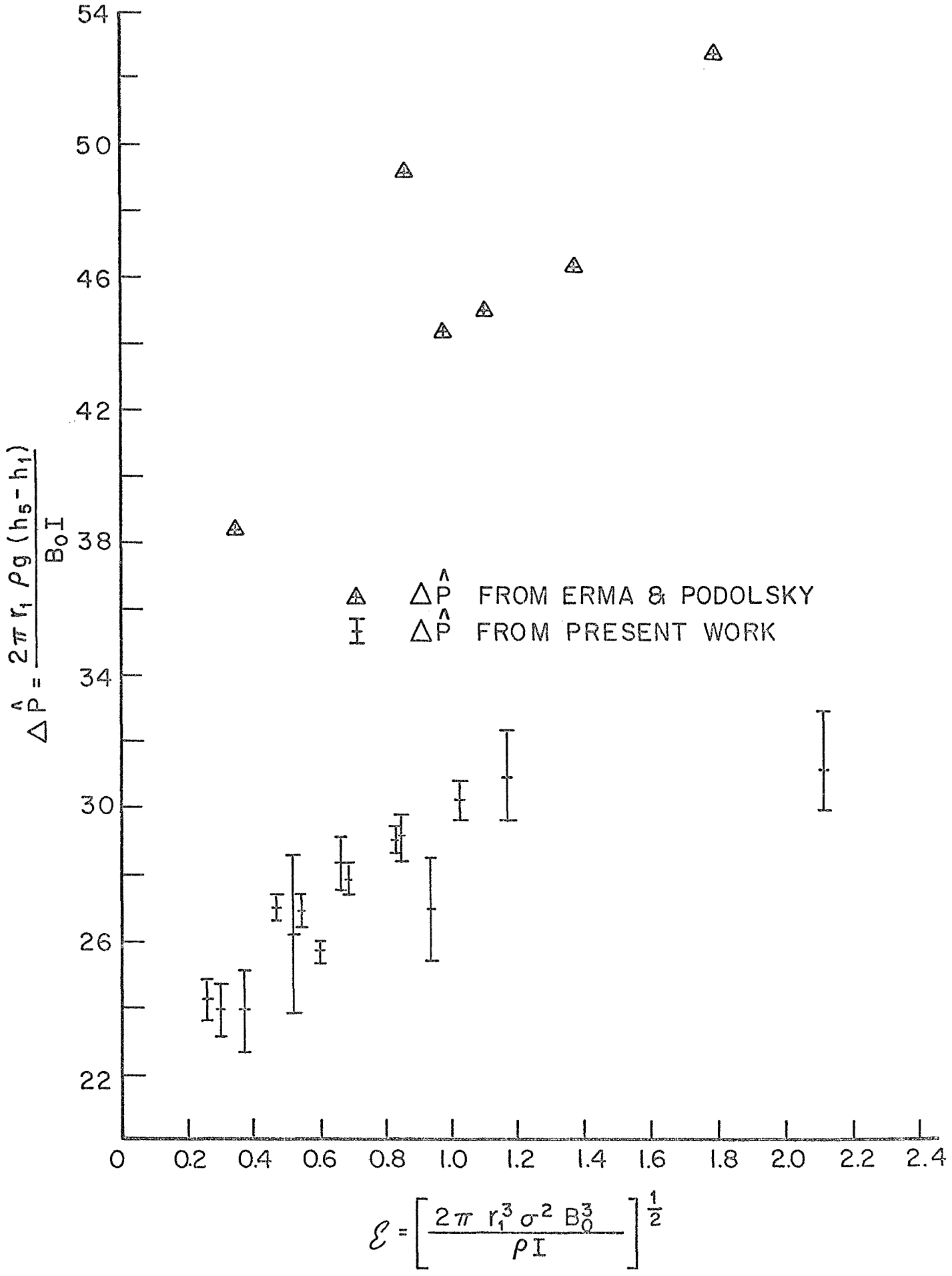
54
50
46
42
38
34
30
26
22
0
0.2
0.4
0.6
0.8
1.0
1.2
1.4
1.6
1.8
2.0
2.2
2.4
$\hat{\Delta P} = \frac{2\pi r_1 \rho g (h_5 - h_1)}{B_0 I}$
$\hat{\Delta P}$ FROM ERMA & PODOLSKY
$\hat{\Delta P}$ FROM PRESENT WORK
$\mathcal{E} = \left[\frac{2\pi r_1^3 \sigma^2 B_0^3}{\rho I}\right]^{\frac{1}{2}}$

FIG. 7